Japanese Journal of Applied Physics

The Japan Society of Applied Physics

REGULAR PAPER • OPEN ACCESS

Finger and stylus discrimination scheme based on capacitive touch screen panel and support vector machine classifier

OPEN ACCESS

Japanese Journal of Applied Physics **58**, 074501 (2019)

REGULAR PAPER

https://doi.org/**10.7567/1347-4065/ab2672**

Finger and stylus discrimination scheme based on capacitive touch screen panel and support vector machine classifier

Ki-Hyuk Seol, Seungjun Park, Seok-Jeong Song, and Hyoungsik Nam*

Dept. of Information Display, Kyung Hee University, Seoul 02447, Republic of Korea

*E-mail: hyoungsiknam@khu.ac.kr

Received April 22, 2019; revised May 27, 2019; accepted June 3, 2019; published online June 17, 2019

This paper demonstrates a support vector machine (SVM) based capacitive touch screen scheme that can discriminate stylus and finger at the same time. The tip of a stylus provides pulses at the higher frequency than the transmitting (Tx) pulse of a touch screen. Then the digital value acquired from an analog-to-digital converter is transferred to an SVM classifier to make the decision of which touch is applied among no-touch, finger-touch, and stylus-touch. Three types of touches are processed on the SVM algorithm. The proposed method is evaluated by means of an 8 inch capacitive touch panel, connector board, Tx/Rx driver board, and host processor board. While Tx pulses are applied at 5 V and 32 kHz that lead to the 200 Hz reporting rate, stylus pulses are produced at 3 V and 315 kHz. The resultant bit error rate is measured as less than 10^{-6} for all types of touches. © 2019 The Japan Society of Applied Physics

1. Introduction

The demands for comfortable and intuitive input methods have been continuously increasing in various devices. Especially, highly durable, sensitive, and multi-touch capable mutual capacitive touch screens have been widely applied to a variety of consumer devices such as smartphones, tablet personal computers, laptop computers, and monitors.[1–4] As shown in Fig. 1, a conventional mutual capacitive touch screen panel (TSP) consists of transmitting (Tx) electrodes and receiving (Rx) electrodes which form some mutual capacitors at their intersection areas.[5,6] Excitation drivers send Tx pulses sequentially that are transferred to charge amplifiers connected to Rx lines through mutual capacitors. These charge amplifier circuits with the connection to a reference voltage (V_{REF}) convert magnitudes of the mutual capacitance into analog voltages. When a finger is touched on the screen, the reduced mutual capacitance is detected as the different output voltage of the charge amplifier from the voltage level without any touches. By and large, to increase the precision of the touch determination, the charge amplifier accumulates the output voltages over multiple Tx pulses. In addition, a multiplexer allows one analog-to-digital converter (ADC) to sample Rx signals sequentially. The digital data are transferred to a host processor to determine the touch positions. The host processor also plays a role to control excitation drivers.

There have been two mainstream TSP researches of improving signal-to-noise ratio (SNR) and adding another input tool such as a stylus except for fingers. Because the sensing performance of TSP is very dependent of SNR at the receiver side, display noises, charger noises, and hum noises should be got to grips with. One of SNR improving technologies is a differential sensing method that cancels out common-mode noises.[7–11] Generally, the adjacent capacitances between the TSP and the display panel are approximately the same. Because it can be assumed that the display noise injected between Rx lines are identical, the differential sensing method can be applied to the TSP very effectively in eliminating display noise. While the conventional method should sense the whole value of mutual capacitance for each crossing area, the differential scheme makes use of just the difference between adjacent capacitances, allowing to increase the output dynamic range of a charge amplifier.

A time-interleaved sensing method reduce the noise by applying multiple Tx pulses per one touch position,[12,13] but lowers the scan rate inevitably. On the other hand, a code-division multiple-sensing (CDMS) method has been introduced to increase SNR as well as scan rate.[14–17] While multiple Tx pulses are used for sensing one touch position like the time-interleaved sensing method, multiple Tx electrodes are excited with orthogonal patterns simultaneously. Then, the touch information over multiple positions can be obtained at the same time through the decoding process. As a result, the CDMS method achieves a much higher scan rate than the time-interleaved sensing method at the same SNR level.

On the other hand, more elaborate input methods than a finger have been studied and developed for handwriting and drawing applications. These needs have been addressed based on the capacitive TSP scheme equivalent to finger-touch sensing or additional TSP technologies. The simplest scheme is a passive stylus whose conductive tip imitates a finger-touch.[18] However, since the contact area must be comparable to that of a finger, it is difficult to fulfill elaborate works. Furthermore, it is impossible to distinguish a stylus from a finger.

Whereas, active stylus schemes can conduct elaborate works with small-sized tips.[19–21] The stylus senses a Tx signal from TSP and re-transmits its inverted and amplified signal to TSP via a tip. Thanks to the process of amplifying the sensed Tx signal, it becomes possible to work with much smaller radius tips than the passive stylus. If larger pulses are applied to the tip, the different output voltage from a finger-touch is obtained at charge amplifiers, which enables the stylus to be differentiated from the finger. However, this requires higher voltage at stylus circuits than Tx pulses to make another voltage level of the stylus detection, which leads to the reduced dynamic range and SNR of the finger detection at the fixed input voltage range of the ADC. As

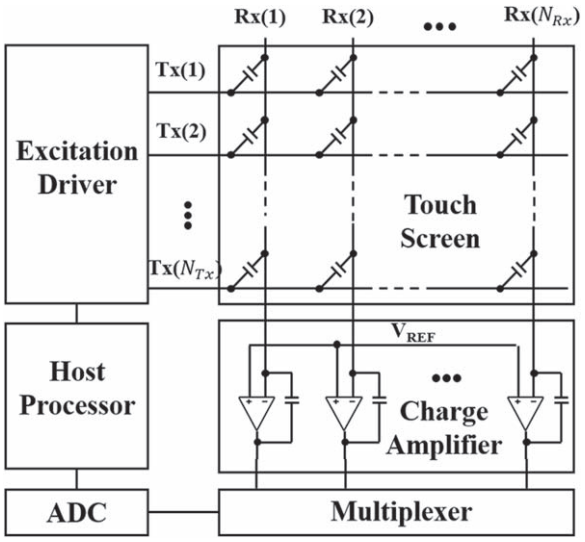

Fig. 1. Block diagram of a conventional touch screen system. N_{Tx} and N_{Rx} are the numbers of transmitting and receiving electrodes, respectively. The capacitors in a touch screen are mutual capacitors at the intersection areas of Tx and Rx lines.

another active stylus method, the stylus generates pulses at a different specific frequency from Tx pulses and TSP is implemented with two separate operation modes of sensing circuitries for finger and stylus-touch events.[22] This method can distinguish the stylus from the finger and maintain SNR as well as dynamic range. But the overall increased complexity in circuits and operations is inevitable because two separate sensing processes are required.

The other active stylus can be used in TSPs with multiple-frequency driving.[23] In addition to being able to find the point of contact by applying a fast Fourier transform (FFT), the finger and the stylus can be distinguished because the stylus and TSP lines are driven at different frequencies. However, in order to implement the FFT functionality, Tx signals must be driven at a very high frequency, which leads to the increased power consumption and hardware complexity.

While previous passive and active ways are grounded in the capacitive TSP, there is a stylus with a different approach that works with an electro-magnetic resonance (EMR) technology.[24] Since EMR responds only to the stylus and the capacitive TSP senses only the finger, two separate touch sensing schemes enable the finger to be distinguished from the stylus. However, this technique needs additional layers that increase hardware complexity as well as manufacturing cost.

This paper presents a capacitive TSP method that can discriminate stylus and finger without adding any layers, increasing operation modes, and reducing dynamic range of the finger-touch detection. Especially, this discrimination is accomplished by the common platform of a support vector machine (SVM) classifier.[25]

2. Proposed SVM-based capacitive TSP

Three kinds of capacitive TSP systems including finger-only touch, conventional active stylus-touch, and proposed active stylus-touch are depicted in Fig. 2. C_M is a mutual capacitor that is created at the crossing area of Tx and Rx lines and arrows represent the directions of electric fields. For the

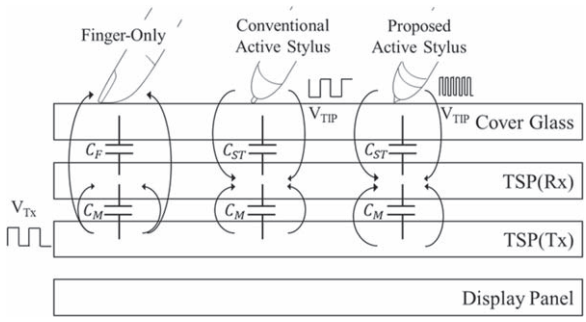

Fig. 2. Cross-sectional views and electric fields of finger-only, conventional active stylus, and proposed active stylus TSP systems.

finger-only touch, because some amount of electric field is taken by the finger, the smaller amount of charges is transferred through C_M to Rx than that without any finger touches. C_F is the parasitic capacitor between Rx line and finger. Whereas, the conventional active stylus senses Tx pulses (V_{Tx}) and re-transmits their inverted and amplified pulses (V_{TIP}) to the TSP. These output pulses of reverse polarities to Tx pulses provide opposite charges via the capacitor (C_{ST}) between the stylus' tip and Rx lines, showing similar effects to finger touches.

While the cross-sectional view of a proposed active stylus scheme is the exactly same as the conventional one, the proposed one gives rise to the higher frequency of V_{TIP} than V_{Tx}. This enables the proposed TSP to discriminate between finger and stylus-touches without the enlarged voltage swing of the stylus output. Unlike the conventional TSP approaches that sense the touch events based on a fixed threshold level, the proposed system thinks of the touch event as a sequence of data samples produced by the ADC for three cases of no-touch, finger-touch, and stylus-touch presented in Fig. 3. In a no-touch case, data samples are obtained at one level with some amount of noises. A finger-touch also generates data samples of one different value from the no-touch. However, the stylus-touch causes the fluctuation on the data sequence due to the higher frequency of V_{TIP} than V_{Tx}. These three cases are explained in more detail along with each charge amplifier circuit schematic.

The no-touch case is simplified into Fig. 4(a) that consists of C_M, a feedback capacitor (C_{FB}), a reset switch (RST) and an operational amplifier (OP-AMP). As shown in Fig. 4(b),

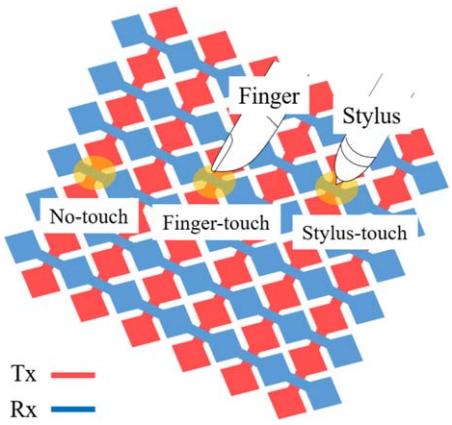

Fig. 3. (Color online) Three cases of no-touch, finger-touch, and stylus-touch for a proposed TSP system.

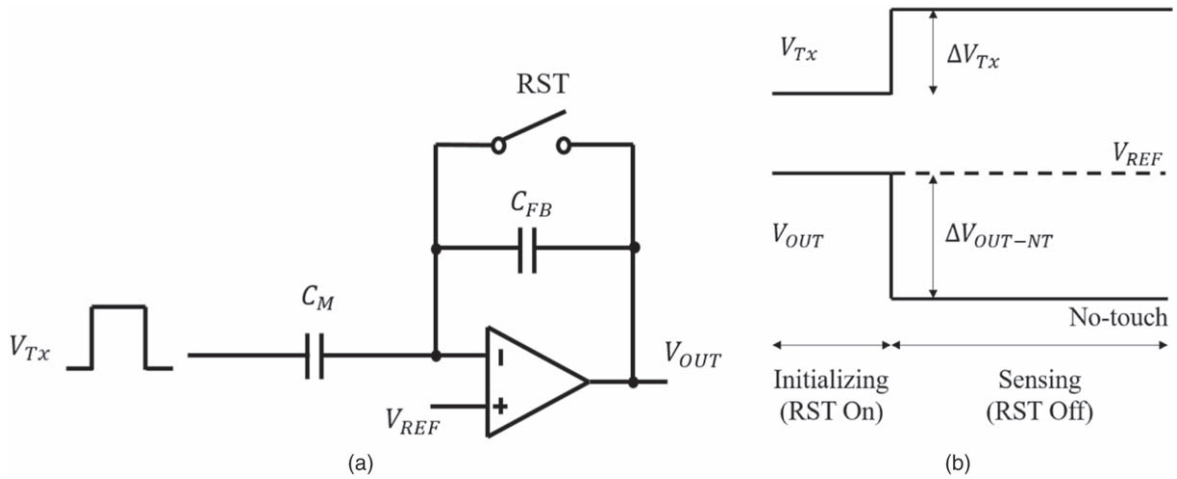

Fig. 4. Rx circuit model for a no-touch case. (a) Charge amplifier circuit schematic (b) waveforms of V_{Tx} and V_{OUT} for two phases of initializing and sensing operations.

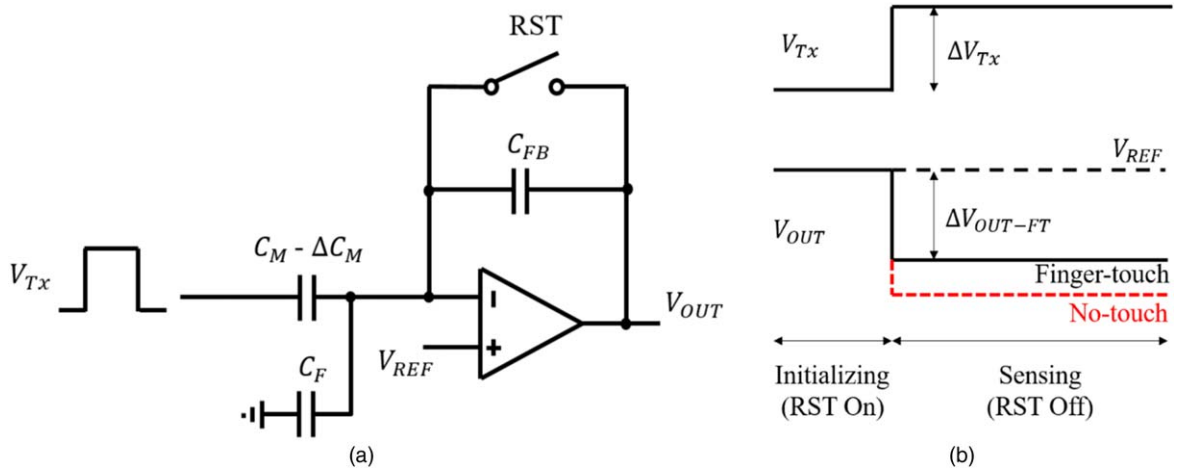

Fig. 5. (Color online) Rx circuit model for a finger-touch case. (a) Charge amplifier circuit schematic (b) waveforms of V_{Tx} and V_{OUT} for two phases of initializing and sensing operations.

the output of the OP-AMP (V_{OUT}) is initialized at V_{REF} by turning RST on during the low period of V_{Tx}. Then, RST is open and V_{Tx} takes the rising transition to change V_{OUT} by $\Delta V_{\mathrm{OUT-NT}}$. $\Delta V_{\mathrm{OUT-NT}}$ is calculated by Eq. (1), depending on voltage swing of V_{Tx} (ΔV_{Tx}), C_{M}, and C_{FB}

$$\Delta V_{\mathrm{OUT-NT}} = \frac{C_{\mathrm{M}}}{C_{\mathrm{FB}}} \times \Delta V_{\mathrm{Tx}}. \tag{1}$$

The finger-touch case is expressed with the reduced capacitance of C_{M} by ΔC_{M} as shown in Fig. 5(a). Since C_{F} is created between Rx line and finger, there are no effects on V_{OUT}. Therefore, the voltage gain ($\Delta V_{\mathrm{OUT-FT}}/\Delta V_{\mathrm{Tx}}$) gets smaller as shown in Eq. (2). $\Delta V_{\mathrm{OUT-FT}}$ is settled at the smaller level than $\Delta V_{\mathrm{OUT-NT}}$ of the no-touch state as depicted in Fig. 5(b)

$$\Delta V_{\mathrm{OUT-FT}} = \frac{C_{\mathrm{M}} - \Delta C_{\mathrm{M}}}{C_{\mathrm{FB}}} \times \Delta V_{\mathrm{Tx}}. \tag{2}$$

Unlike two previous touch cases, a proposed stylus-touch can be modeled by adding a capacitor (C_{ST}) between stylus and Rx line as presented in Fig. 6(a). It is assumed that as the radius of a tip is small enough, there is no reduction on the mutual capacitance. V_{TIP} has a higher frequency than V_{Tx} to generate ripples of ΔV_{ST} on V_{OUT} during the sensing period as illustrated in Fig. 6(b). The maximum possible swing level of ΔV_{ST} ($\Delta V_{\mathrm{ST}}^{\mathrm{max}}$) is shown in Eq. (3) with ΔV_{TIP} that is the amplitude of V_{TIP} pulses

$$\Delta V_{\mathrm{ST}}^{\mathrm{max}} = \frac{C_{\mathrm{ST}}}{C_{\mathrm{FB}}} \times \Delta V_{\mathrm{TIP}}. \tag{3}$$

A timing diagram of ADC sampling operations is shown in Fig. 7 by depicting $V_{\mathrm{OUT-NT}}$, $V_{\mathrm{OUT-FT}}$, and V_{ST} according to V_{Tx} and V_{TIP} . Blue dotted lines indicate the voltage level in the case of no-touch state, and green dotted lines indicate the voltage level in the case of the finger-touch state. Red dots in $V_{\mathrm{OUT-NT}}$, $V_{\mathrm{OUT-FT}}$, and V_{ST} are the sampling points when the ADC samples the charge amplifier outputs at the middle point of the sensing phase. Especially, V_{TIP} is supported as free running pulses at a higher frequency than Tx pulses only when V_{Tx} is asserted at the high level. When V_{OUT} is sampled by the following ADC and the frequencies of V_{Tx} and V_{TIP} have no relationship of a factor of an integer, the data sequence of the stylus-touch shows the fluctuation unlike the constant data sequences of no-touch and finger-touch as shown in Fig. 8. Therefore, the stylus can be detected without any additional voltage levels,

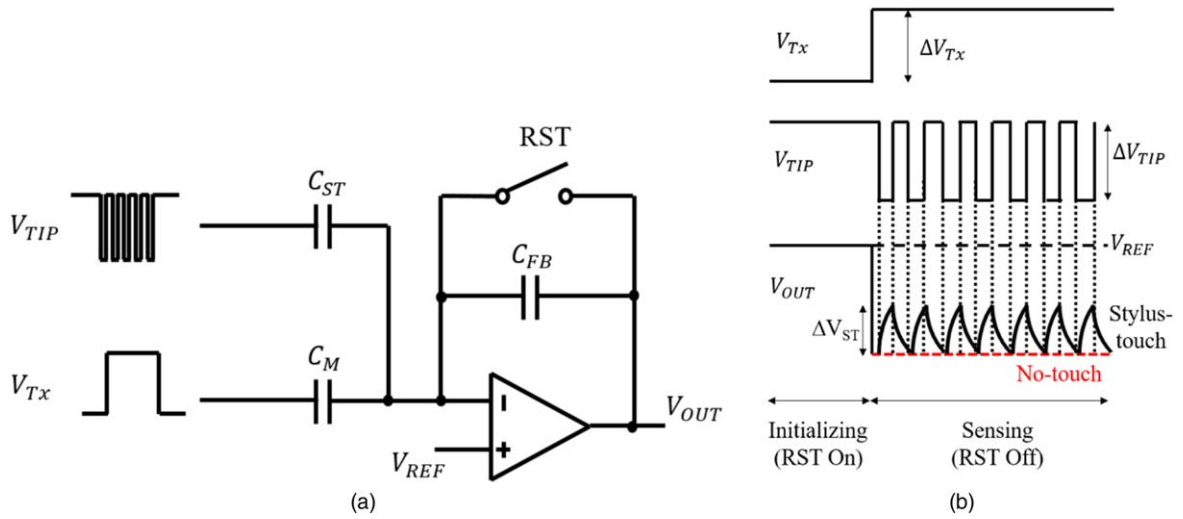

Fig. 6. (Color online) Rx circuit model for a stylus-touch case. (a) Charge amplifier circuit schematic (b) waveforms of V_{Tx}, V_{TIP}, and V_{OUT} for two phases of initializing and sensing operations.

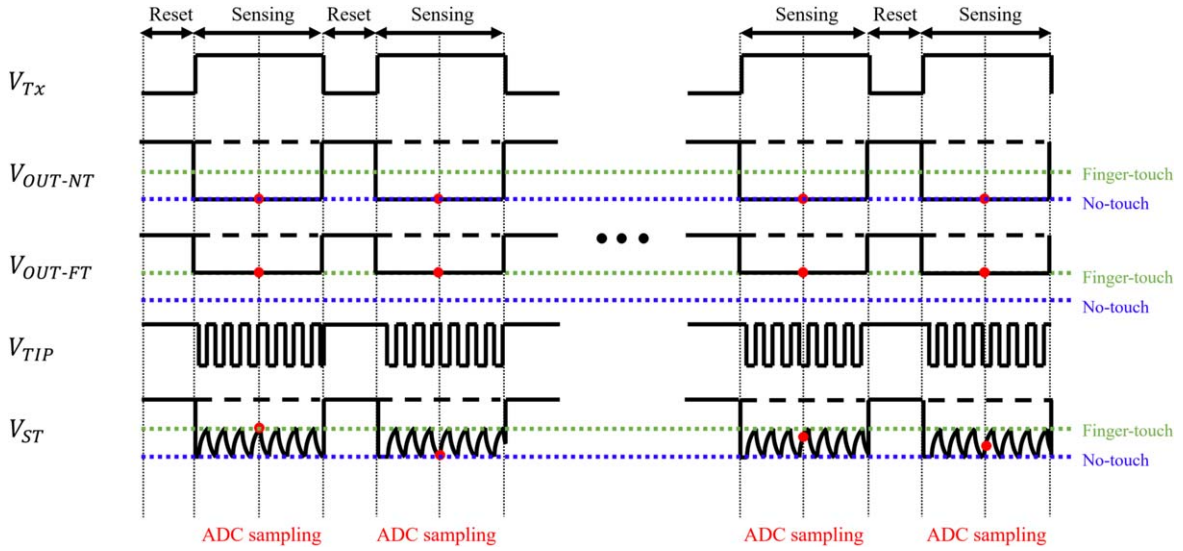

Fig. 7. (Color online) ADC sampling operations for three touch cases. Red dots represent sampling points at charge amplifier outputs.

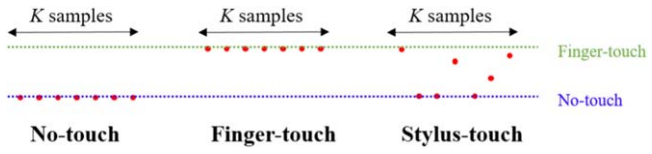

Fig. 8. (Color online) Data sequences for three touch cases after ADC sampling.

maintaining the dynamic range of the finger-touch detection.

The data sequence of K samples is transferred to the host processor where the received sequence is classified into one of three touch cases by means of the SVM algorithm. SVM is one of the most commonly used machine learning algorithms for classification. SVM focuses on the problem to find the decision boundary for dividing the space with respect to the margin maximization.[26] The margin is defined as the minimum distance between the boundary and any of samples. Therefore, it requires only the small portion of samples that are close to the boundary, that is, the support vectors. The high dimension space has the hyperplane boundaries. Furthermore, SVM can have the nonlinear hyperplane boundaries with various kernel functions such as polynomial and Gaussian. Groups of data can be classified by finding a subset of data points called support vectors so that the distance between two groups of data points is maximized comparing the distance between these support vectors.[27] Because SVM usually achieve higher performance compared to other classification methods, we used a SVM classifier to discriminate three touch states. No-touch and finger-touch lead to features of different constant value from each other and the stylus-touch makes features of fluctuating values. Accordingly, three cases are distinguishable. However, since the SVM is basically a two-class algorithm, the one-versus-the-rest method is employed to discriminate three classes as depicted in Fig. 9. After the data sequence is handled by three SVMs from SVM1 to SVM3, the most possible one among them is selected as a final output at a rating block. For example, if a finger is placed on a screen, SVM1 and SVM3 present that samples are not for no-touch and stylus-touch

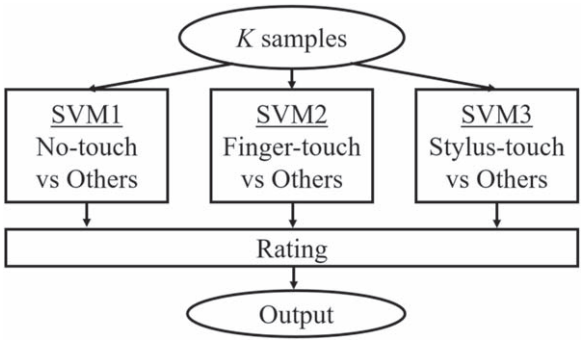

Fig. 9. One-versus-the-rest SVM classification scheme for the proposed touch system.

cases, and SVM2 shows that they are for a finger-touch case. Finally, the classification result is determined as a finger-touch.

As a consequence, the classification for three cases is accomplished by one common SVM algorithm without any modifications in threshold, sensing circuit, and algorithm.

3. Experimental results

The overall evaluation system consists of 8 inch capacitive touch panel, connector board, Tx/Rx driver board, and host processor board as presented in block diagram and photography of Figs. 10(a) and 10(b). For the touch panel of this evaluation setup, one Tx line is driven and one Rx line is sensed to verify the proposed touch sensing technology. A connector board provides the contact point of a Rx line and includes a level shifter integrated circuit to drive the Tx line at 5 V.[28] A Tx/Rx driver board that is implemented with a programmable system-on-chip evaluation board (Cypress Semiconductor PSoC 5LP) gives rise to Tx pulses of 3.3 V and senses the voltage sequence of a Rx line by means of a charge amplifier with C_{FB} of 3 pF and 8-bit ADC. The mutual capacitance of a cross area between a Tx line and a Rx line is estimated as 1.8 pF from Eq. (1) with C_{FB} of 3 pF, ΔV_{Tx} of 5 V, and measured ΔV_{OUT-NT} of 3 V. The stylus capacitance of a cross area between a tip and a Rx line can also be estimated as 0.4 pF from Eq. (3) with C_{FB} of 3 pF, ΔV_{TIP} of 3 V, and measured ΔV_{ST} of 0.4 V. Through a universal serial bus (USB), the digitally converted data are transferred to a host processor board that runs the SVM algorithm to differentiate three touch modes. A Raspberry Pi board (Raspberry Pi Foundation Raspberry Pi 3) is used as a host processor board.

The number of samples (K) for SVM is 16 and support vectors are extracted from 3×10^6 training data sequences that are 10^6 sequences for each touch case. N_{Tx} and N_{Rx} that are the numbers of Tx and Rx lines are assumed to be 20 and 16, respectively.[28] The frequency of Tx pulses (f_{Tx}) is 32 kHz that leads to 100 Hz reporting rate as described in Eq. (4). 32 kHz is determined by considering the maximum data rate that can be supported by the USB modules in PSoC board and Raspberry Pi board. Because the number of

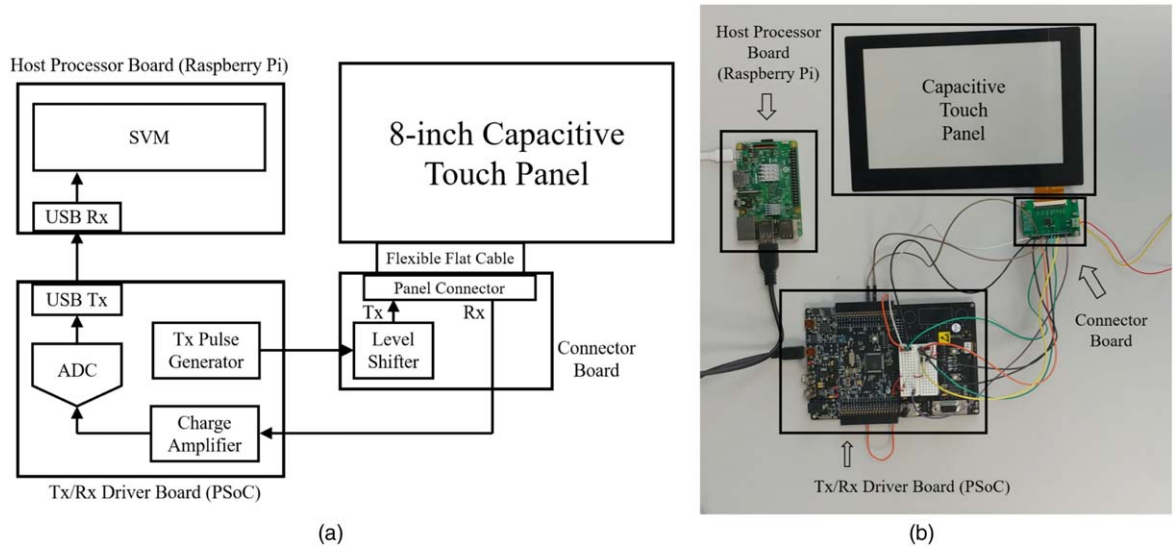

Fig. 10. (Color online) Evaluation setup of a proposed touch system. (a) Block diagram (b) photography.

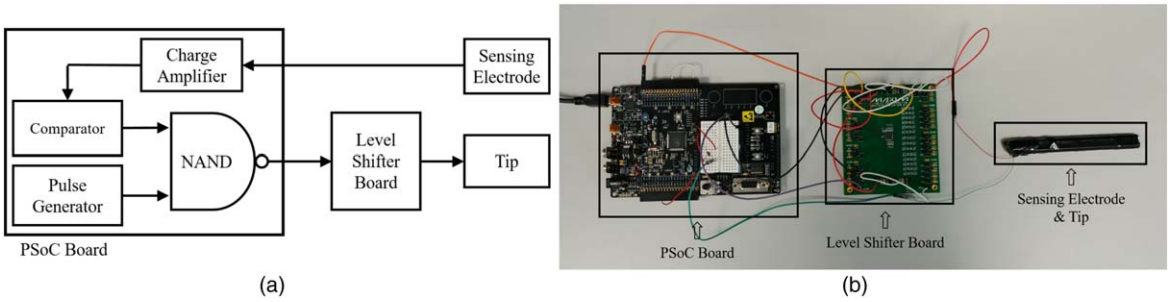

Fig. 11. (Color online) Proposed stylus emulation system. (a) Block diagram (b) photography.

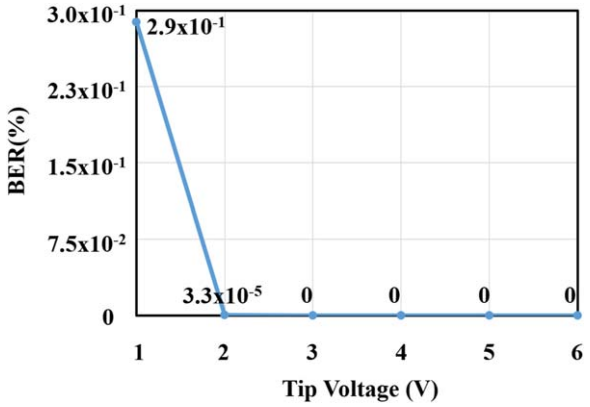

Fig. 12. (Color online) Measured BERs for tip voltages from 1 to 6 V when the length of data sequence (K) is 16.

extracted support vectors are 25 and their dimensions are equal to K, the proposed SVM classifier can be implemented by the simple matrix multiplication of support vector matrix of $25 \times K$ and input matrix of $K \times N_{Rx}$ for intersection points of one Tx line. At the 3.30 GHz central processing unit environment, all intersection points of 20 Tx and 16 Rx lines are processed within 1 ms that is equivalent to the reporting rate of 1000 Hz

$$\text{Reporting rate} = \frac{f_{\text{Tx}}}{K \times N_{\text{Tx}}} = \frac{32\,000}{16 \times 20} = 100(\text{Hz}). \quad (4)$$

Unlike previous approaches,[8,11,28] the reporting rate of the proposed one is independent of N_{Rx} because all Rx lines are sampled by one ADC of the high sampling rate (f_{ADC}) for a Tx pulse. The sampling rate is obtained as Eq. (5) where the factor of 2 is added with consideration of the 50% duty ratio of the Tx pulse. If the higher duty ratio is in use, the resultant smaller factor than 2 can lead to the reduction on the sampling rate. In this evaluation setup, since this evaluation is conducted for one Rx line, the ADC samples the output voltage of the charge amplifier at 32 kHz that is the same frequency as f_{Tx}

$$f_{\text{ADC}} = f_{\text{Tx}} \times N_{\text{Rx}} \times 2 = 1.024(\text{MHz}). \quad (5)$$

To emulate a proposed stylus, a tip and a sensing electrode are made of iron nails with a diameter of 5 mm. A PSoC board amplifies the sensed Tx pulses that are used as an input of a NAND gate with the output of a pulse generator to produce the tip voltage. The voltage level at a tip is controlled by a level shifter evaluation board (Maxim Integrated MAX17079) and the frequency was set at 315 kHz, which

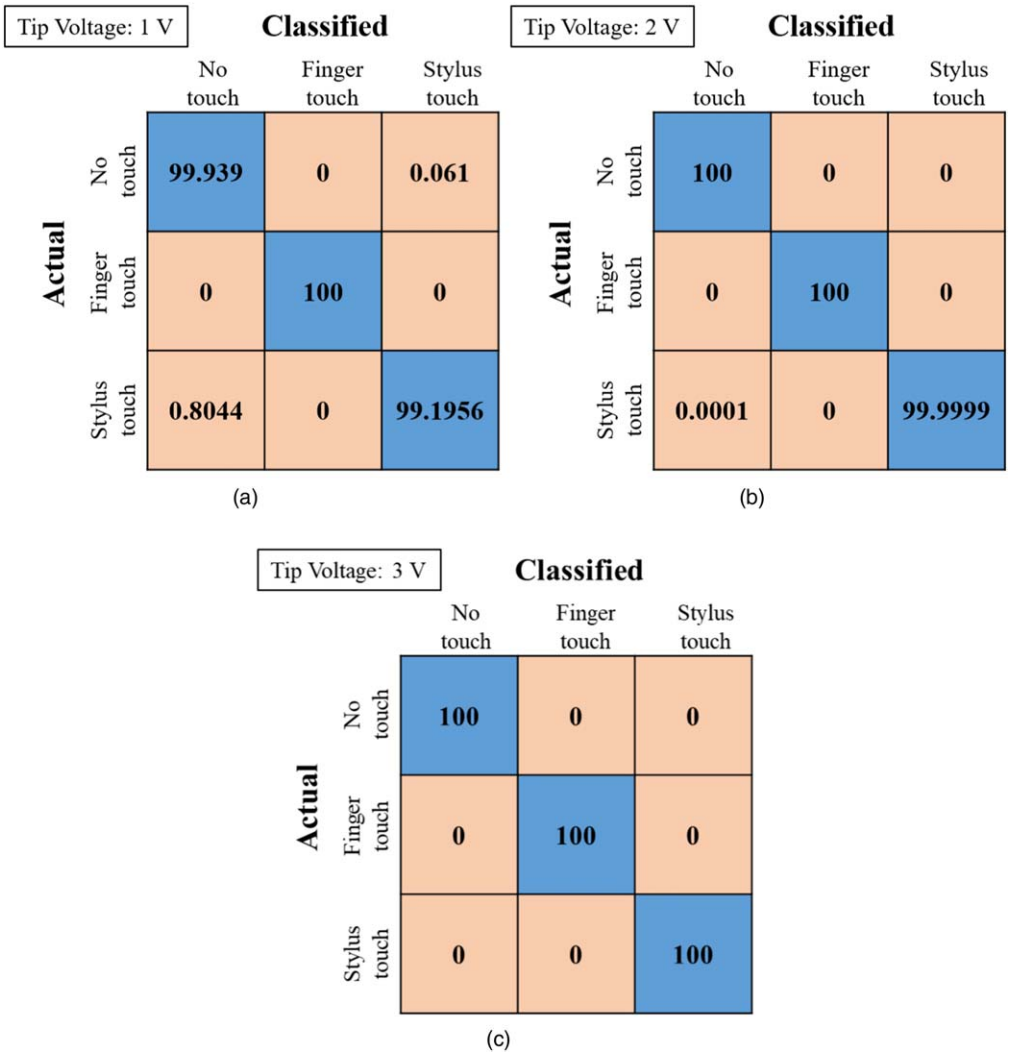

Fig. 13. (Color online) Confusion matrices in the unit of% for the touch SVM classifier. (a) 1 V tip voltage (b) 2 V tip voltage (c) 3 V tip voltage.

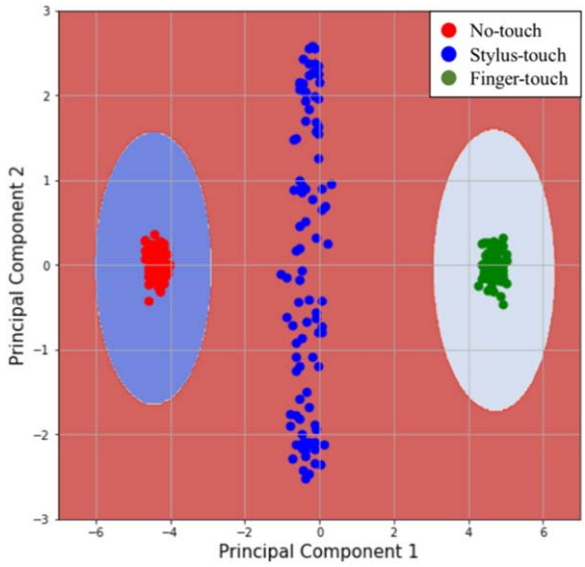

Fig. 14. (Color online) Decision boundaries of SVM for two principal components at K of 16 and ΔV_{TIP} of 3 V.

is not related to Tx by an integer multiple. The block diagram and photography are shown in Figs. 11(a) and 11(b).

To determine the tip voltage level, bit error rates (BERs) for 10^6 sequences are measured over the voltage range from 1 to 6 V as plotted in Fig. 12. Especially, confusion matrices for tip voltages of 1, 2, and 3 V are illustrated in Figs. 13(a)–13(c). The blue areas show the accuracy of the SVM classifier and the remaining areas are the misclassified cases. The values are presented in%. While the low voltage of 1 V misclassifies some stylus-touches and no-touches, the high voltages of 2 V and 3 V achieve very one and zero misclassified cases, respectively. Zero misclassification means less BER than 10^{-6} for all three touches. Therefore, 3 V is determined as a tip voltage in this evaluation. In addition to BERs, the decision boundaries are visualized only with two largest principal components in Fig. 14 because the 16-dimensional original data are impossible to visualize. These two principal components are extracted by two largest variance components to approximate a high dimensional space into a low dimensional one in the principal component analysis.[26] Due to the Gaussian kernel function, the nonlinear boundaries are established.

Three measured output waveforms for no-touch, finger-touch, and stylus-touch events are presented in Figs. 15(a)–15(c). The output voltage changes for no-touch and finger-touch are 3 and 2.6 V. In particular, the stylus-touch shows the ripples within 2.6 and 3 V during sensing periods.

As shown in Fig. 16(a), both finger and stylus are put on the screen to verify that the proposed scheme can discriminate two touches. A tack connected to the ground is used as the finger-touch. Two touches are placed on the same Rx line (Rx1) but on different Tx lines (Tx1, Tx2). Figure 16(b) shows measured BERs when the finger and stylus are simultaneously contacted to the screen over the tip voltage of 1–6 V. The similar result to Fig. 12 is achieved. As a consequence, it is ensured that two touch tools of finger and stylus are successfully discriminated by the proposed SVM-based method. This stylus and finger discrimination enables the user-friendly stylus interface such as palm-rejection. Typically, when the user wants to write something with the stylus, the palm of a hand touches the screen of the device. If the touch screen cannot distinguish the stylus from the palm-touch handled as the finger-touch, it would be very inconvenient to use the stylus. On the other hand, our proposed TSP system can support palm-rejection by detecting the stylus and rejecting the palm-touch information at the same time.

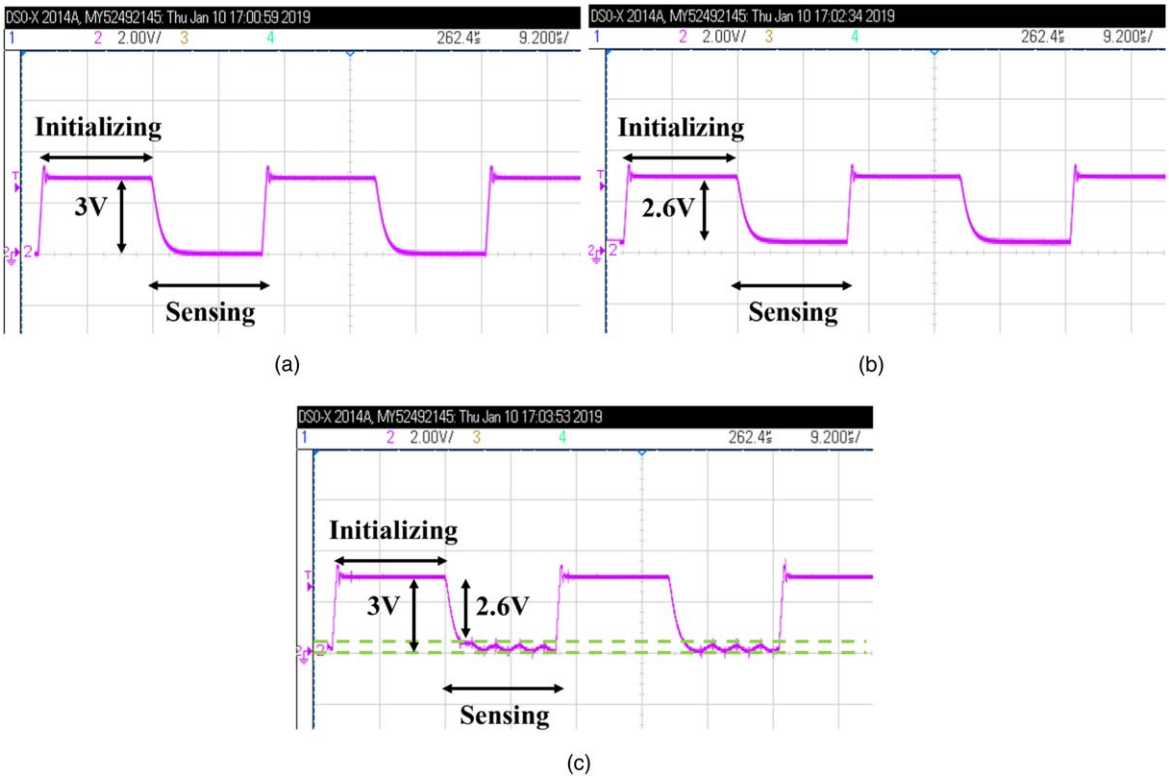

Fig. 15. (Color online) Measured output waveforms for the charge amplifier. (a) No-touch, (b) finger-touch (c) stylus-touch.

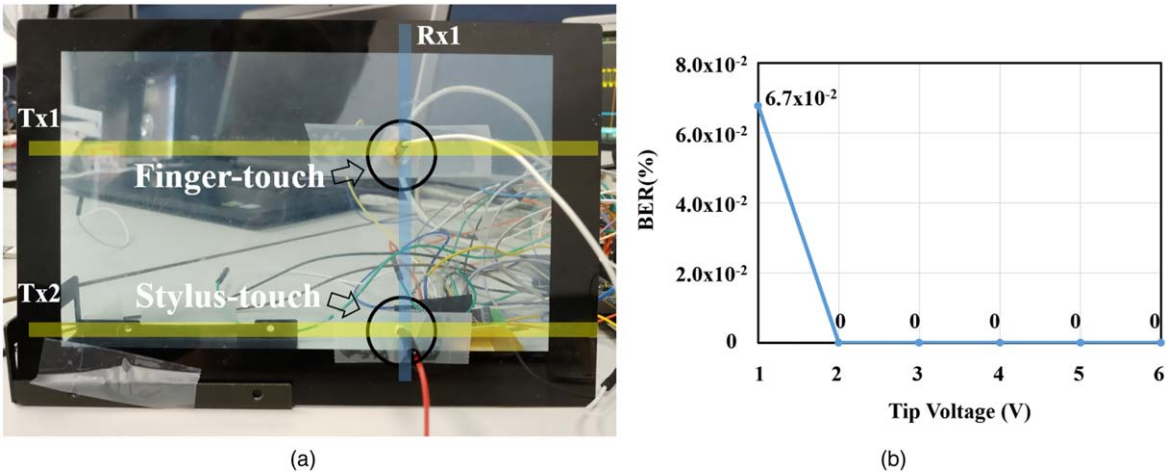

Fig. 16. (Color online) Discrimination of finger and stylus when both touches are placed on the screen at the same time. (a) evaluation setup photography (b) measured BERs for tip voltages from 1 to 6 V.

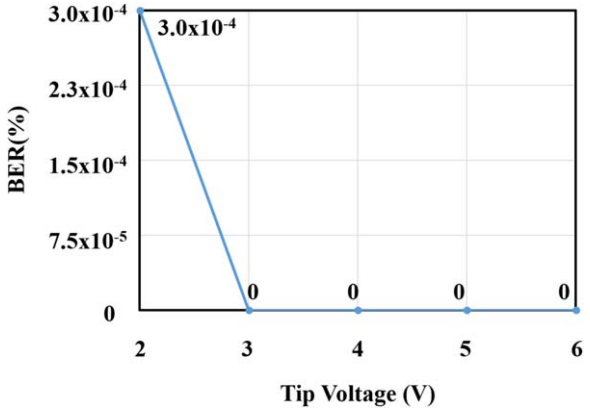

Fig. 17. (Color online) Measured BERs for tip voltages from 2 to 6 V when the length of data sequence (K) is 8.

On the other hand, to increase the reporting rate further up to 200 Hz, the length of data sequence K should be reduced to 50%. Thus, the tip voltages of a stylus are evaluated again regarding BERs at K of 8. The measured BERs are plotted in Fig. 17, showing that the 200 Hz reporting rate can be established by a similar tip voltage of 3 V for BER $<10^{-6}$. However, it should be recognized that at a tip voltage of 2 V, the proposed SVM classifier shows higher BER in K of 8 than in K of 16. K is the number of samples that is equal to the dimension of the input data for our SVM classifier. It is well-known that as the dimensionality of the data increases, the volume of the space increases exponentially.[26] Therefore, the distance between three touch cases in that K-dimensional space becomes more distant as K increases. Consequently, the BER for 8-dimensional samples is higher than for 16-dimensional ones regarding the same environment.

4. Conclusion

This paper proposes a finger and stylus discrimination scheme that is based on capacitive touch screen technology and an SVM classification algorithm. Unlike previous approaches, because the sequence of samples on Rx lines are classified by SVM, three cases of no-touch, finger-touch, and stylus-touch are discriminated on the common platform without any additional threshold voltage levels. To generate the differentiable sequence for a stylus, the frequency of a tip voltage is set to be higher than Tx pulses. This work supports stylus-touch along with palm-rejection that is the discrimination of stylus and finger, requires no increase in hardware complexity, and maintains dynamic range, compared to conventional finger-only TSPs.

Acknowledgments

This research was supported by IDEC (EDA Tool) and the National Research Foundation of Korea (NRF) funded by the Ministry of Science, ICT & Future Planning (NRF-2016R1A2B4009787).

ORCID iDs

Hyoungsik Nam https://orcid.org/0000-0002-1646-7954

1) N.-H. Yu et al., Proc. ACM SIGCHI, 2011, p. 2995.
2) C. Park, S. Park, K.-D. Kim, S. Park, J. Park, B. Kang, Y. Huh, and G.-H. Cho, IEEE J. Solid-State Circuits **51**, 168 (2016).
3) J. Seo and H. Nam, IEEE J. Electron Devices Soc. **6**, 726 (2018).
4) Y. Chen, D. Geng, and J. Jang, IEEE J. Electron Devices Soc. **6**, 214 (2018).
5) T.-H. Hwang, W.-H. Cui, I.-S. Yang, and O.-K. Kwon, IEEE Trans. Consum. Electron. **56**, 1115 (2010).
6) C. Luo, M. A. Borkar, A. J. Redfern, and J. H. McClellan, IEEE Trans. Emerg. Sel. Top. Circuits Syst. **2**, 639 (2012).
7) I.-S. Yang and O.-K. Kwon, IEEE Trans. Consum. Electron. **57**, 1027 (2011).
8) J.-H. Yang, S.-H. Park, J.-M. Choi, H.-S. Kim, C.-B. Park, S.-T. Ryu, and G.-H. Cho, IEEE ISSCC Dig. Tech. Pap. (2013), p. 390.
9) B. Li, T. Wei, X. Wei, J. Wang, W. Liu, and R. Zheng, J. Disp. Technol. **12**, 646 (2016).
10) S. Heo, H. Ma, J. Song, K. Park, E.-H. Choi, J. J. Kim, and F. Bien, IEEE Trans. Circuits Syst. I **63**, 960 (2016).
11) S.-H. Park, H.-S. Kim, J.-S. Bang, G.-H. Cho, and G.-H. Cho, IEEE J. Solid-State Circuits **52**, 528 (2017).
12) N. Miura, S. Dosho, H. Tezuka, T. Miki, D. Fujimoto, T. Kiriyama, and M. Nagata, IEEE J. Solid-State Circuits **50**, 2741 (2015).
13) H. Xing, L. Deng, J. Ke, T. Yu, C. Liao, H. Luo, and S. Huang, IEEE Sens. J. **19**, 1412 (2018).
14) M. Miyamoto and K. Iizuka, "Linear device value estimating method, capacitance detection method, integrated circuit, touch sensor system, and electronic device," U.S. Patent 8,942,937 (2015).
15) H. Shin, S. Ko, H. Jang, I. Yun, and K. Lee, IEEE ISSCC Dig. Tech. Pap. (2013), p. 388.

16) M. Hamaguchi, A. Nagao, and M. Miyamoto, IEEE ISSCC Dig. Tech. Pap. (IEEE, Piscataway, NJ, 2014), p. 214.
17) S.-L. Huang, S.-Y. Hung, and C.-P. Chen, IEEE Access **7**, 3980 (2019).
18) M. Badaye and R. R. Schediwy, "Passive stylus for capacitive sensors," U.S. Patent 8,125,469 (2012).
19) S. Vuppu, D. Cranfill, M. Olley, and M. Valentine, "Active stylus for use with touch-sensitive interfaces and corresponding method," U.S. Patent 8,766,954 (2014).
20) S. Shahparnia, K. Sundara-Rajan, Y. Ali, and I. Bentov, "Active stylus with high voltage," U.S. Patent 8,866,767 (2014).
21) M. Vlasov, "Active stylus for touch sensing applications," U.S. Patent 9,158,393 (2015).
22) R. Zachut, "Digitizer, stylus and method of synchronization therewith," U.S. Patent 8,481,872 (2013).
23) J.-S. An et al., IEEE ISSCC Dig. Tech. Pap. (2017), p. 168.
24) C. Chang-Hsien and C.-H. Huang, "Method for sensing fast motion, controller and electromagnetic sensing apparatus," U.S. Patent App. 14/472,345 (2015).
25) J. Vavrek, J. Juhar, and A. Cizmar, Proc. IEEE Int. Conf. Telecommun. and Signal Process., 2013, p. 512.
26) C. Bishop, *Pattern Recognition and Machine Learning* (Springer, New York, 2007).
27) S.-J. Song and H. Nam, Displays **53**, 54 (2018).
28) J.-H. Yang, S.-H. Park, J.-Y. Jeon, H.-S. Kim, C.-B. Park, J.-C. Lee, J.-W. Kim, and G.-H. Cho, SID Symp. Dig. Tech. Pap. **43**, 1570 (2012).